Korean J. Chem. Eng., 34(3), 854-865 (2017)
DOI: 10.1007/s11814-016-0304-2

pISSN: 0256-1115
eISSN: 1975-7220

Optimization of supercritical extraction of galegine from *Galega officinalis L.*: Neural network modeling and experimental optimization via response surface methodology

Pooya Davoodi, Seyyed Mohammad Ghoreishi†, and Ali Hedayati

Department of Chemical Engineering, Isfahan University of Technology, Isfahan 84156-83111, Iran
(*Received 23 August 2016 • accepted 24 October 2016*)

Abstract−Supercritical CO_2 extraction of galegine from *Galega officinalis L.* was carried out under different operating conditions of temperature (35-55 °C), pressure (10-30 MPa), dynamic extraction time (30-150 min), CO_2 flow rate (0.5-2.5 mL/min) and constant static extraction time of 20 min. Design of experiment was by response surface methodology (RSM) using Minitab software 17. The response surface analysis accuracy was verified by the coefficient of determination (R^2=93.4%) along with modified coefficient of determination (mod-R^2=87.7%). The optimum operating conditions were found by using RSM modeling to be 42.8 °C, 22.7 MPa, 141.5 min and 2.15 mL/min, in which the maximum galegine extraction yield of 3.3932 mg/g was obtained. Artificial neural network (ANN) using Levenberg-Marquardt backpropagation training function with six neurons in the hidden layer was implemented for the modeling of galegine extraction such that the coefficient of determination (R^2) was 96.6%.

Keywords: Supercritical Extraction, *Galega officinalis L.*, Artificial Neural Network (ANN), Response Surface Methodology (RSM), Galegine

INTRODUCTION

The use of plants as therapeutic tools has played a remarkable role in the popular medicine of different countries [1]. *Galega officinalis L.*, commonly called Gout's Rue, is a member of legume family (Fabaceae), that is native to southern Europe and Western Asia. *G. officinalis L.* grows along stream banks and in moist areas, preferring full sun, but tolerating light shade [2-5].

G. officinalis L. is prescribed as an anti-diabetic and a diuretic agent [6]. The therapeutic potential of *G. Officinalis L.* for the management of diabetes was defined in the first half of the 20th century [7-10]. Additionally, there are some more studies that show the effect of *G. officinalis L.* extract on human platelet aggregation [10] and body weight [11].

Galegine was first isolated from this plant by Tanret [12] and recognized as a guanidine derivate, (3-methylbut-2-en-ethyl) guanidine, by Spath and Perkop [3]. Several other constituents were also obtained, namely 4-hydroxy galegine, alkaloid, peganine, flavones, tannins, saponin, sucrose, and fatty oils [13]. Galegine reduces the blood glucose level [14], has anticoagulation effects [15], lowers the blood pressure [16] and increases milk production in sheep [17]. Therefore, galegine extraction from *G. officinalis L.* and its characterization is an important research area.

Extraction and purification of *G. officinalis L.* essential oils by conventional methods has been done [18]. Common extraction methods such as hydro and steam distillation have several disadvantages, such as incomplete extraction from plant materials, high operating temperatures with the consequent breakdown of thermally labile components, promotion of hydration reactions of chemical constituents and requirement of a post-extraction process for water removal [19-21]. Solvent extraction overcomes the drawbacks of distillation, but has the major disadvantage of solvent residue in the extracts [22,23].

In the past two decades, there has been an increasing interest in supercritical fluids (SCF) resulting from potential application in chemical, petrochemical, pharmaceutical, environmental and food industries [24-27]. Supercritical fluid processes have specific characteristics that make them attractive as solvents. In particular, solvent density, and hence solvent effectiveness can be controlled by pressure and temperature, and liquid-like densities and gas-like viscosities, coupled with diffusion coefficients that are at least an order of magnitude higher than those of liquids, contribute to enhancement of mass transfer [28-30]. Although there are many components which can be used in SCF processes, carbon dioxide (CO_2) is the most popular solvent for SCF extraction studies, primarily because of its low critical temperature and pressure. Furthermore, supercritical carbon dioxide (SC-CO_2) is inert, pure, nontoxic, environmentally friendly, inexpensive and gaseous under ambient conditions. Thus, the solute separation, concentration process and drying process are made easier and the generation of liquid solvent waste and exposure of operators to toxic solvents can be minimized [31-33].

To the best of our knowledge, there is not any published data in the literature regarding supercritical extraction of galegine from *Galega officinalis L.* plant matrix. Thus, the main objective of this research was the optimization of galegine extraction from *G. officinalis L.* using SC-CO_2 as a solvent in periodic static-dynamic procedure for pharmaceutical application. The optimization was carried

†To whom correspondence should be addressed.
E-mail: ghoreshi@cc.iut.ac.ir

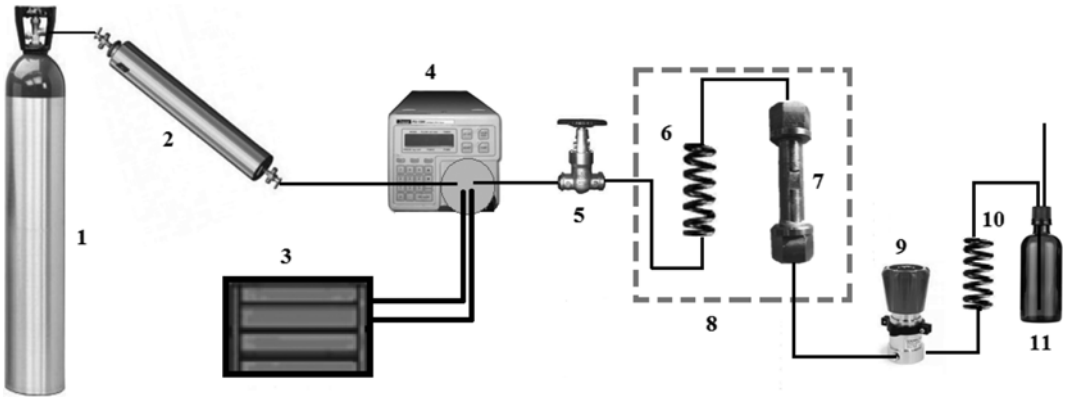

Fig. 1. The experimental setup for the supercritical extraction system.

1. CO_2 cylinder
2. Molecular sieve column
3. Cooler
4. HPLC pump
5. Needle valve
6. Coil preheater
7. Extraction column
8. Oven
9. Back pressure regulator
10. Restrictor heater
11. Collection vial

out by response surface methodology (RSM), which is an effective and powerful method for optimizing experimental conditions and investigation of critical processes while reducing the number of experimental trials [34-36]. RSM is useful for modeling, problem analysis and optimization when a response is influenced by several variables such as pressure, temperature, flow rate of SC-CO_2 and dynamic time. In the current work the other effective variable, static time, was fixed at an optimum value of 20 min that was obtained by experiment. On the other hand, artificial neural network (ANN) modeling (MLP: multi-layer perceptron) was developed for simulating SC-CO_2 extraction of galegine from *G. officinalis L.* matrix. ANN eliminates the limitations of the classical approaches and is a good alternative to conventional empirical modeling. The simplifying assumptions in the mathematical modeling of supercritical extraction problems decrease the model accuracy and validity. Therefore, heuristic models based on experimental results have been proposed to estimate the required data and avoid excessive experiments [37,38].

EXPERIMENTAL

1. Materials

Galega officinalis L. was obtained from Zard Band Company which produces raw materials for pharmaceutical producers. Leaves were dried at room temperature for 30 days prior to the experimental studies. The dried samples were stored inside a sealed bag in a cold and dry place until use. Commercial grade carbon dioxide (CO_2 purity>97%) was purchased from ZAMZAM Co. (Isfahan, Iran). Galegine (purity of 98%, Select Lab. Co.) was purchased to use in liquid chromatography-mass spectrometry (LC-MS) analysis. Ethanol (99.99%, Bidestan Company, Iran) was used as the conventional solvent for extraction.

2. Soxhlet Extraction

The extraction was carried out using ethanol as solvent (350 mL), which was heated to reflux. The solvent (ethanol) vapor traveled up the distillation arm and flooded into the thimble of solid (20 g of dried *Galega officinalis*). The condenser ensures that any solvent vapor cools, and drips back down into the chamber housing. The chamber containing dried *Galega officinalis* slowly filled with warm ethanol. When the Soxhlet chamber became almost full, the chamber was emptied by a siphon. The solvent was returned to the distillation flask. The thimble ensures that the rapid motion of the solvent does not transport any solid material to the still pot. This cycle lasted 8 hours. During each cycle, a portion of the non-volatile compound dissolved in the ethanol. After many cycles the desired compound (galegine) was concentrated in the distillation flask. The advantage of this system is that instead of many portions of warm solvent being passed through the sample, just one batch of solvent was recycled. After extraction, the solvent was removed. Total galegine content of *G. officinalis L.* leaves was determined to be 3.4120 mg/g.

3. Supercritical Fluid Extraction: Apparatus and Procedure

The extraction experiments involved using a custom built high-pressure extractor apparatus. Fig. 1 shows a schematic of the extraction apparatus. To use CO_2 which was stored in cylinder with highest purity it was passed through a molecular sieve beads column. Then, CO_2 was cooled to $-5\,^{\circ}C$ in a heat exchanger that used ethylene-glycol as coolant, and subsequently charged by a feed pump (HPLC pump, Jasco). The needle valve which had been placed between discharge stream of pump and coil preheater was completely closed during static extraction time and completely opened in dynamic extraction time process. Coil preheater located in the oven was employed to heat CO_2 before entering the extraction column. The system pressure was controlled with an accuracy of ±0.5 Mpa and monitored by a high-pressure pump and back-pressure regulator (Tescom, 10,000 psi). At the effluent of back pressure regulator, a restrictor heater increases the temperature of exit stream up to $70\,^{\circ}C$ to avoid freezing problems due to Joule-Thompson effects. The stainless-steel column (height=12.5 cm, inner diameter (i.d.)= 0.9 cm, and outer diameter (o.d.)=1.3 cm) fitted with cotton wool at the effluent was manually charged with fine powder of *G. officinalis L.* leaves (2.5 g) and glass beads with a mesh size of 18-35 (1-1.5 mm).

The extraction procedure consisted of static (batch mode) and dynamic periods of extraction. A 20 min static extraction period was employed to increase sample-solvent contact time. After static

extraction time, dissolved components were discharged from the extraction column by passing CO_2 at different flow rates and then trapped and collected with 15 mL of ethanol in collection vial. Eventually, the yield was determined as displayed in Eq. (1).

$$\text{Extraction Yield (mg/g), E.Y.} = \frac{\text{Mass of extracted } \textit{Galegine} \text{ (mg)}}{\text{Mass of dried } \textit{G. officinalis} \text{ leaves (g)}} \quad (1)$$

4. Sample Analysis

Pure standard galegine and extracted galegine samples were analyzed and quantified by liquid chromatography-mass spectrometry (LC-MS) apparatus. The Thermo Scientific HPLC column (100× 2.1 mm packed with 5 μm biobasic-4 solid phase) was used with mobile phase and mobile phase velocity of 20 mM Ammonium acetate in methanol and 0.3 mL/min, respectively. The mass spectrometry conditions were capillary voltage of 23 V, capillary temperature, 250 °C, and vaporizer temperature, 450 °C. The calibration curve was plotted by injection of different concentration of solutions made by standard galegine with linear regression R^2=0.968 and retention time: 6.8 min. The concentrations of galegine in extracted samples were obtained by linear calibration curve according to y= 1106x−371.5. Fig. 2 shows the chromatogram for pure standard galegine and one of the extracted samples in supercritical fluid extraction, respectively.

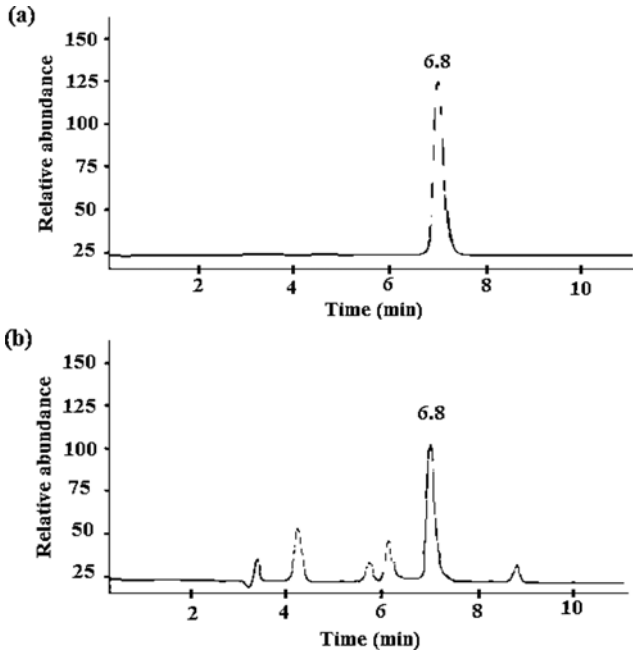

Fig. 2. (a) Chromatogram of pure standard galegine, (b) chromatogram of galegine in the SFE extracted sample.

THEORY

1. Response Surface Methodology

The objectives of using RSM can be explained through four main goals: (1) reducing amount of experimentation needed, (2) ensuring adequate range of variation in all operating parameters (3) minimizing confounding of effects, and (4) ensuring that one finds causal relationships rather than just correlations [39-41].

Therefore, the extraction method described in the above section was optimized by using an experimental design. A central composite design (CCD) was employed to collect data by four factors and five levels of variable combinations and determine the optimal factors of Extraction Yield (EY). Because it is not possible to identify the effects of all parameters, it is necessary to select the parameters that have major effects [42]. According to preliminary experiments, the range of four independent and most effective variables, namely temperature (Z_1), pressures (Z_2), extraction time (Z_3) and flow rate (Z_4), were chosen in the range of 35-55 °C, 10-30 MPa, 0.5-2.5 mL/min and 30-150 min, respectively. The experimental data of different levels of factors are shown in Table 1.

In this research, 31 different combinations, including 16 Cube points, 8 Axial points to form a central composite design and 7 replications for the center point (each signed the coded value (0, 0, 0, 0)), were chosen in random order according to a CCD (α=1.72) configuration to minimize the effects of unpredicted variability in the observed responses due to irrelevant factors. A second-order polynomial regression model was employed to express EY as a function of the input variables as follows [43,44]:

$$\text{E.Y.}=A_0+A_1X_1+A_2X_2+A_3X_3+A_4X_4+A_{11}X_1^2+A_{22}X_2^2+A_{33}X_3^2+A_{44}X_4^2 + A_{12}X_1X_2+A_{13}X_1X_3+A_{14}X_1X_4+A_{23}X_2X_3+A_{24}X_2X_4+Z_{34}X_3X_4+\varepsilon \quad (2)$$

where EY, dependent variable, is the predicted response of total galegine extraction yield (mg/g), A_0, A_i, A_{ii} and A_{ij} are constant and the linear, squared, and interaction coefficients of the model, in that order. In addition, ε is an error term that depicts the sources

Table 1. Uncoded and coded levels of independent variables used in RSM design

Coded-variables levels	Independent variable			
	Temperature (T) (°C)	Pressure (P) (MPa)	Flow rate (F) (mL/min)	Extraction time (t) (min)
Z_i	X_1	X_2	X_3	X_4
1.72 (+α)	53.6	28.6	2.36	141.6
1	50	25	2	120
0 (central point)	45	20	1.5	90
−1	40	15	1	60
−1.72 (−α)	36.4	11.4	0.64	38.4
$\Delta\xi$	5	5	0.5	30

of variability not be captured by polynomial equation. It is assumed that ε's over different runs are independent, and have mean zero. Z_i and Z_j are input variables in coded forms defined according to the following equation [45]:

$$Z_i = \frac{X_i - X_{i,\,cp}}{\Delta\xi} \tag{3}$$

Finally, MINITAB 17 was used for designing experiments, fitting, and statistical data analysis (ANOVA) of obtained data. The accuracy of the model was evaluated by the coefficient of determination (R^2) using the following equation:

$$R^2 = 1 - \frac{\Sigma_{i=1}^{n}(y_i - \hat{y}_i)^2}{\Sigma_{i=1}^{n}(y_i - \bar{y})^2} \tag{4}$$

where y_i, $\hat{y}_i$, $\bar{y}$ and n are experimental data, predicted data, average of experimental data, and number of experiment respectively.

2. Artificial Neural Networks

Artificial neural networks (ANNs) are highly simplified models of the structure of a biological network, simulating analytical functions of the human brain. An artificial neuron, or simply a neuron, is the fundamental processing element of ANN. These networks have an innate ability to learn and identify highly non-linear multivariable systems with any complexity by experience and experiment without any prior assumptions about their nature and interrelations to be used in many scientific disciplines [46]. ANNs have been successfully applied in many scientific applications due to the ability to solve complicated problems by extracting the desired information using the input data. This modeling technique uses the experimental inputs for the prediction of the required data to avoid the need for additional experiments [47-49].

In an ANN, neurons are located in a series of layers: 1- Neurons representing independent variables are in the input layer; 2- neurons representing dependent variables are in the output layer and 3- multiple hidden layers. These neurons sum the weighted inputs and then apply a transfer function to the sum while each neuron is connected to other neuron in the next layer.

The pattern of interconnection among the neurons is called the network architecture. Multi-layer perceptron (MLP) network architecture is the generally used feed-forward topology (architecture) of ANN which uses back-propagation learning algorithm [50,51]. Fig. 3 shows the MLP network, which consists of an input layer with four neurons, an output layer with one neuron, and one hidden layer with six neurons, while each connecting line corresponds to a certain weight. The inputs for the network include pressure, temperature, extraction time and CO_2 flow rate and the output is the extraction yield of galegine. Minimizing the network error function by adjusting these weights is done for the network training.

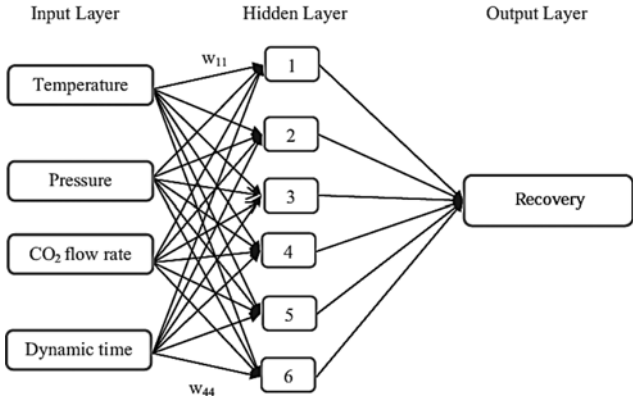

Fig. 3. Schematic diagram of the neural network structure for SC-CO_2 extraction of galegine.

As indicated in Eq. (5), a neuron output resulting from applying a transfer function to a weighted summation of its input, serves as input to other neurons [52,53].

$$\gamma_{jk} = F_k\left(\sum_{i=1}^{N_{k-1}} W_{ijk}\gamma_{i(k-1)} + \beta_{jk}\right) \tag{5}$$

where β_{jk} is the bias weight for neuron j in layer k and γ_{jk} is the neuron j's output from k's layer. The model-fitting parameters (W_{ijk}), are the connection weights that were selected randomly and F_k is the nonlinear activation transfer functions.

The MLP network contains a three-stage iterative process: 1- weights and biases approximation and output values evaluation; 2- error calculation, and 3- updating the weights. The final performance of the network depends on the network structure, training method and of the initial value assigned to the weights.

We used MLP network with three layers (six neurons in the hidden layer) using Levenberg-Marquardt backpropagation training function to calculate the galegine extraction. Also, logistic sigmoid $f(x)=1/(1+e^{-ax})$ and purelin ($f(x)=x$) transfer functions were selected for hidden and output layers, respectively. The MLP network with three layers and enough number of neurons in the hidden layer is appropriate for the modeling of system based on Kolmogorov theorem [54].

Inputs and output were normalized in the range of 0-1 to reduce the network error and increase homogeneous results using Eq. (6) [52,53]:

$$X_{norm} = \frac{X - X_{min}}{X_{max} - X_{min}} \tag{6}$$

where X_{norm}, X, X_{min}, and X_{max} are normalized value, actual value, minimum value, and maximum value, respectively.

RESULTS AND DISCUSSION

1. Fitting the Model and Analysis of Experimental Data

The effects of four operation variables on supercritical extraction of galegine were investigated using RSM with central composite design (CCD); the results of model predictions in different operating conditions are presented in Table 2. The regression coefficients are summarized in Table 3, and the significance of each coefficient was determined by absolute t-value and p-value, which are listed in the same table. For any of the terms in the model, a large absolute value of t and a small p-value would indicate more significant effects on the corresponding response variables. In this research, model terms with $p<0.001$, $0.001\leq p<0.05$ and $p\geq 0.05$ are highly significant, significant and insignificant, respectively. The second-order polynomial model for galegine yield (E.Y.) was obtained as a function of independent variables:

Table 2. Experimental and predicted data for the yield of galegine obtained from CCD

Run no.	Coded variable				Process variable				Experimental yield (mg/g×100)	Predicted yield (mg/g×100)
	Z_1 (T)	Z_2 (P)	Z_3 (F)	Z_4 (t)	X_1	X_2	X_3	X_4		
1	−1	−1	−1	−1	40.0	15	1.00	60.0	334.70	335.13
2	1	−1	−1	−1	50.0	15	1.00	60.0	337.51	337.41
3	−1	1	−1	−1	40.0	25	1.00	60.0	336.98	336.65
4	1	1	−1	−1	50.0	25	1.00	60.0	337.59	337.94
5	−1	−1	1	−1	40.0	15	2.00	60.0	336.25	336.36
6	1	−1	1	−1	50.0	15	2.00	60.0	337.17	337.34
7	−1	1	1	−1	40.0	25	2.00	60.0	338.47	338.55
8	1	1	1	−1	50.0	25	2.00	60.0	338.13	338.53
9	−1	−1	−1	1	40.0	15	1.00	120.0	338.22	337.69
10	1	−1	−1	1	50.0	15	1.00	120.0	338.67	338.74
11	−1	1	−1	1	40.0	25	1.00	120.0	338.98	338.96
12	1	1	−1	1	50.0	25	1.00	120.0	339.26	339.02
13	−1	−1	1	1	40.0	15	2.00	120.0	337.51	337.31
14	1	−1	1	1	50.0	15	2.00	120.0	336.85	337.05
15	−1	1	1	1	40.0	25	2.00	120.0	339.26	339.24
16	1	1	1	1	50.0	25	2.00	120.0	338.27	337.99
17	−1.72	0	0	0	36.4	20	1.50	90.0	337.53	337.81
18	1.72	0	0	0	53.6	20	1.50	90.0	339.04	338.70
19	0	−1.72	0	0	45.0	11.4	1.50	90.0	336.63	336.54
20	0	1.72	0	0	45.0	28.6	1.50	90.0	338.63	338.66
21	0	0	−1.72	0	45.0	20	0.64	90.0	337.57	337.78
22	0	0	1.72	0	45.0	20	2.36	90.0	338.23	337.96
23	0	0	0	1.72	45.0	20	1.50	38.4	338.40	337.74
24	0	0	0	1.72	45.0	20	1.50	141.6	338.89	339.48
25	0	0	0	0	45.0	20	1.50	90.0	339.04	339.04
26	0	0	0	0	45.0	20	1.50	90.0	339.01	339.04
27	0	0	0	0	45.0	20	1.50	90.0	339.10	339.04
28	0	0	0	0	45.0	20	1.50	90.0	338.97	339.04
29	0	0	0	0	45.0	20	1.50	90.0	339.12	339.04
30	0	0	0	0	45.0	20	1.50	90.0	338.99	339.04
31	0	0	0	0	45.0	20	1.50	90.0	339.05	339.048

Table 3. Regression coefficients and corresponding standard error, *t* and *p*-values for galegine yield

Coefficient	Term	Effect	Values	S.E. coefficient	*t*-Value	*P*-value*
A_0	Constant		339.048	0.13796	2459.064	0.000
A_1	T	0.5181	0.2590	0.08026	3.228	0.005
A_2	P	1.2319	0.6160	0.08026	7.675	0.000
A_3	F	1.1036	0.0518	0.08026	0.645	0.528
A_4	t	1.0095	0.5048	0.08026	6.289	0.000
A_{11}	T^2	−0.5347	−0.2673	0.08864	−3.016	0.008
A_{22}	P^2	−0.9775	−0.4888	0.08864	−5.514	0.000
A_{33}	F^2	−0.7950	−0.3975	0.08864	−4.485	0.000
A_{44}	t^2	−0.2913	−0.1457	0.08864	−1.643	0.120
A_{12}	T×P	−0.4950	−0.2475	0.09393	−2.635	0.018
A_{13}	T×F	−0.6525	−0.3262	0.09393	−3.473	0.003
A_{14}	T×t	−0.6150	−0.3075	0.09393	−3.274	0.005
A_{23}	P×F	0.3300	0.1650	0.09393	1.757	0.098
A_{24}	P×t	−0.1275	−0.0638	0.09393	−0.679	0.507
A_{34}	F×t	−0.8100	−0.4050	0.09393	−4.312	0.001

*$p<0.001$, highly significant; $0.001<p<0.05$, significant; $p<0.05$, not significant

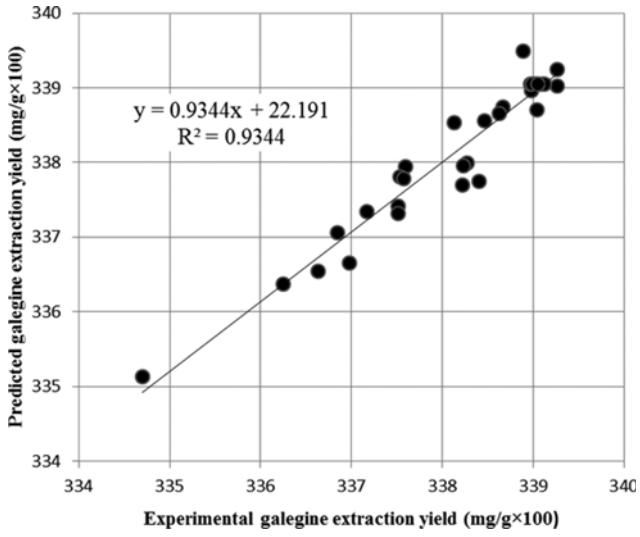

Fig. 4. Predicted values (RSM) versus experimental (observed) values for galegine yield.

$$E.Y.=339.048+0.2590\times T+0.6160\times P+0.5048\times t-0.2673\times T^2 -0.4888\times P^2-0.3975\times F^2-0.2575\times T\times P-0.3262\times T\times F -0.3075\times T\times t+0.1650\times P\times F-0.0638\times P\times t-0.4050\times F\times t \quad (7)$$

Therefore, the linear terms of three independent variables (temperature, pressure, and extraction time) have had the largest effect on the galegine yield. The quadratic term of all parameters, except extraction time and the interaction between temperature and pressure, temperature and extraction time, temperature and flow rate as well as flow rate and extraction time, had also considerable effects on the yield.

The predicted yield values versus experimental values are shown in Fig. 4, which shows the coefficient of determination, R^2=0.934 and AAD=0.06%. The average absolute deviation error (AAD) was calculated according to the following equation:

$$AAD\% = \frac{1}{NP}\sum_{i=1}^{NP}\left|\frac{R_{exp,\,i}-R_{model,\,i}}{R_{exp,\,i}}\right|\times 100 \quad (8)$$

2. Optimization of Extraction Operating Conditions

Working in optimum condition creates an economical process. Hence, to scale up a process from laboratory to commercial plant, optimization is completely necessary. The maximum efficiency of a process will occur when independent variables are in their optimum conditions. Thus, based on the illustrated model, Eq. (7), the most favorable condition for the highest galegine yield was obtained to be at T=42.8 °C, P=22.7 MPa, F=2.15 mL/min, and t=141.5 min, while the yield was 3.3932 mg/g under this condition. The accuracy of the modeling maximum galegine recovery was validated with triplicate experiments at the optimal operating conditions giving the average extraction yield of 3.3930±0.0010 mg/g. Fig. 5 shows the optimal operating condition for extraction of galegine from *Galega officinalis L.* based on coded variables.

3. Response Surface Analysis

The interactions among different variables were investigated by a three-dimensional response surface model according to Eq. (7). The plots were designed by sketching the galegine extraction yield (response: z-axis) versus two independent variables (x and y coordinates), and the other two independent variables were considered constant at zero levels.

3-1. Effect of Temperature

Figs. 6-8 show that changing temperature had two counter influences on the extraction yield.

Increasing the temperature leads to lower SC-CO_2 density and higher galegine vapor pressure. When the vapor pressure of solute dominates, the solubility increases by increasing the temperature. But, as the effect of SC-CO_2 density overcomes the effect of solute vapor pressure, the solubility of galegine decreases due to the lower solvation power of SC-CO_2 and decreases the extraction yield.

As illustrated in Table 3, temperature had a significant ($0.001\leq p<0.05$) positive linear effect and a significant negative quadratic effect, while the interaction of temperature-pressure, temperature-flow rate and temperature-time also had a significant effect on galegine extraction yield. When the operating parameters (pressure, dynamic time and flow rate) are in their optimum values, increasing temperature from 35 °C (code=−1.720) to 42.8 °C (code=−0.4343) leads to more extraction yield (the positive effect of tem-

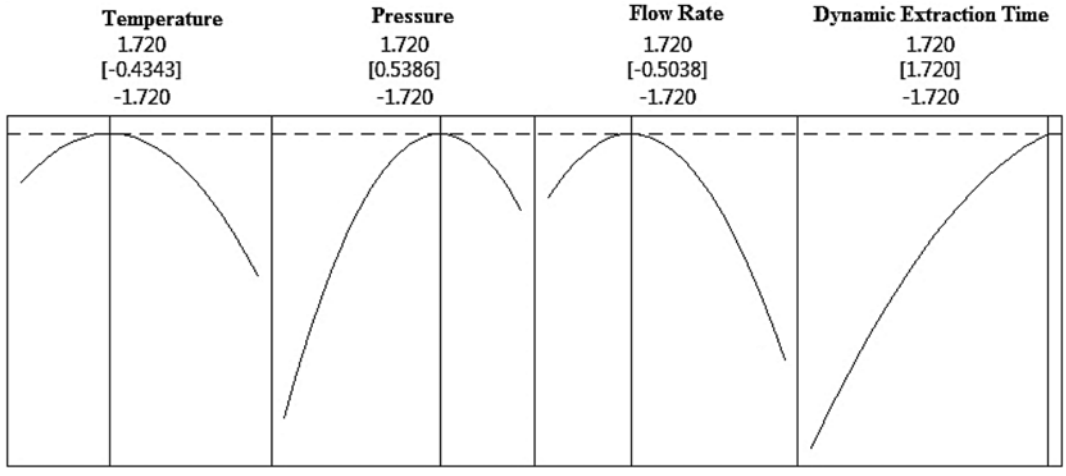

Fig. 5. Optimum operating conditions according to the coded variables based on RSM.

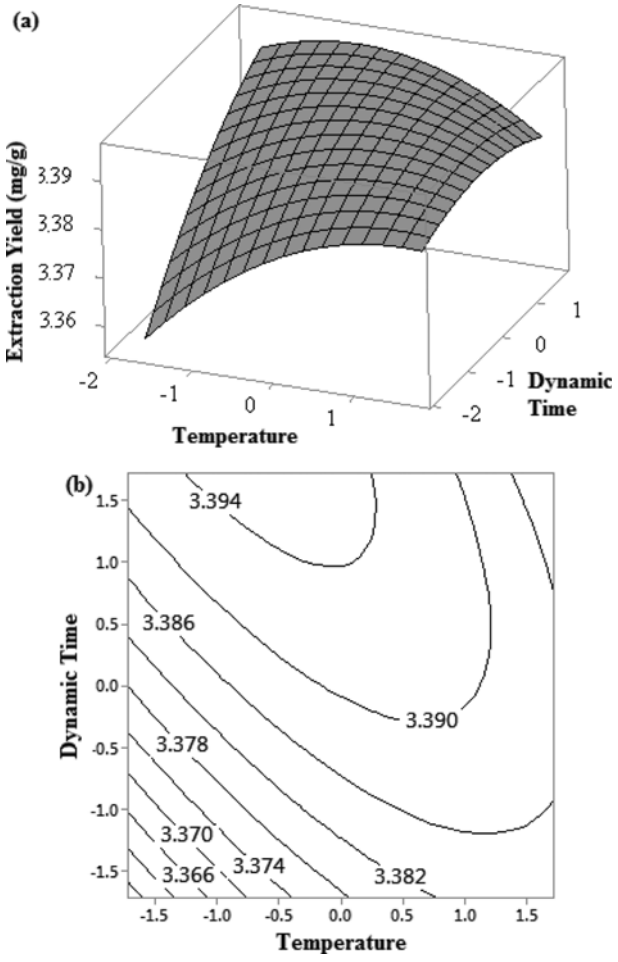

Fig. 6. The effects of temperature and dynamic extraction time (coded values) on the galegine yield at CO_2 flow rate of 1.5 mL/min and pressure of 20 MPa, (a) response surface plot, (b) contour plot.

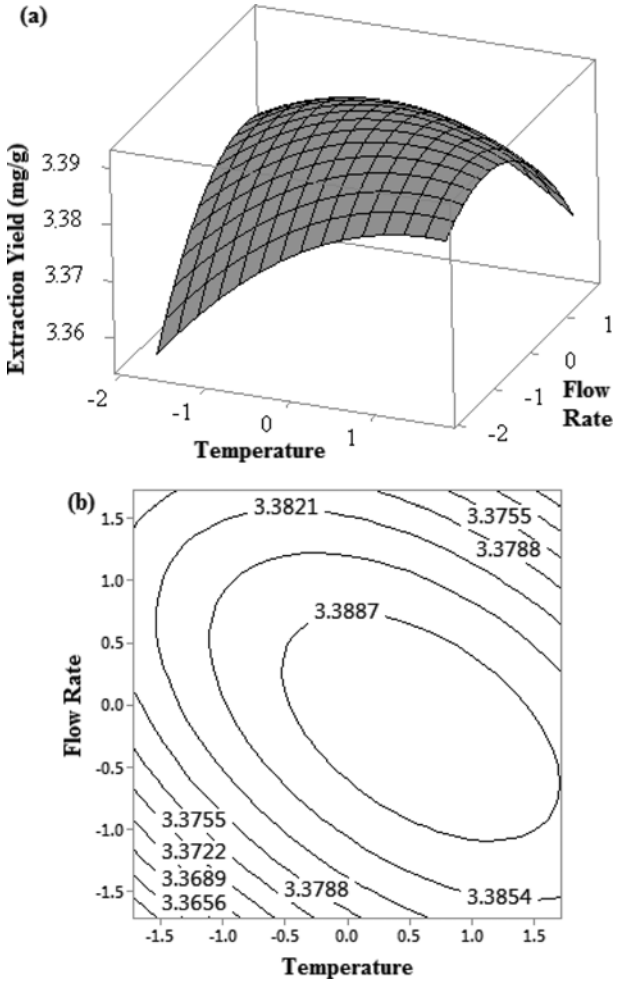

Fig. 7. The effects of temperature and CO_2 flow rate (coded values) on the galegine yield at pressure of 20 MPa and dynamic extraction time of 90 min, (a) response surface plot, (b) contour plot.

perature with enhanced mass transfer coefficient, diffusivity and solute vapor pressure is more dominant than the negative effect of temperature with lower SCF density), but further increasing the temperature from 42.8 °C (code=−0.4343) to 55 °C (code=1.720) leads to lower recovery of galegine extraction.

The phenomenon of retrograde solubility was reached at the optimal temperature (42.8 °C) where the dual counter effects are equal. Beyond that the negative effect of temperature was more important and resulted in the reduction of extraction yield.

3-2. Effect of Pressure

Solute (galegine) solubility in supercritical CO_2 improves with increasing the pressure because of higher SC-CO_2 density and solvation power. On the other hand, the galegine diffusivity and convective mass transfer coefficient decrease at higher pressures. Table 3 shows that pressure had highly significant ($p<0.001$) linear positive effect and quadratic negative effect. All interaction terms of pressure with other parameters were insignificant ($p>0.05$) except the interaction between pressure and temperature (as stated in section 4.3.1).

At the optimum condition, by increasing operating pressure from 10 MPa (code=−1.72) to 22.7 MPa (code=1.27), overwhelming positive effect of increased SC-CO_2 density improved the galegine extraction yield. Increasing repulsive solute-solvent interactions resulting from the highly compressed CO_2 at high-pressure levels and decreasing permeability and mass transfer coefficient with further increasing the pressure (from 22.7 MPa (code=0.5386) to 30 MPa (code=1.72)) prevailed the increasing effect of density and galegine extraction yield was decreased. Thus, the highest recovery was obtained at almost 22.7 MPa (code=0.5386) according to Section 4.2. Figs. 8-10 illustrate the effect of pressure on the galegine extraction yield.

3-3. Effect of Flow Rate

The effect of CO_2 flow rate on the extraction yield versus temperature, pressure and dynamic extraction time is shown in Figs. 8, 10 and 11. The speed of supercritical fluid flowing through the extraction vessel could have two opposite influences on the yield. The slower flow rate of CO_2 results in deeper penetration of solvent, and subsequently leads to complete interaction with solid matrix. But its negative effect is lower mass transfer rate since concentration gradient become negligible. On the other hand, exter-

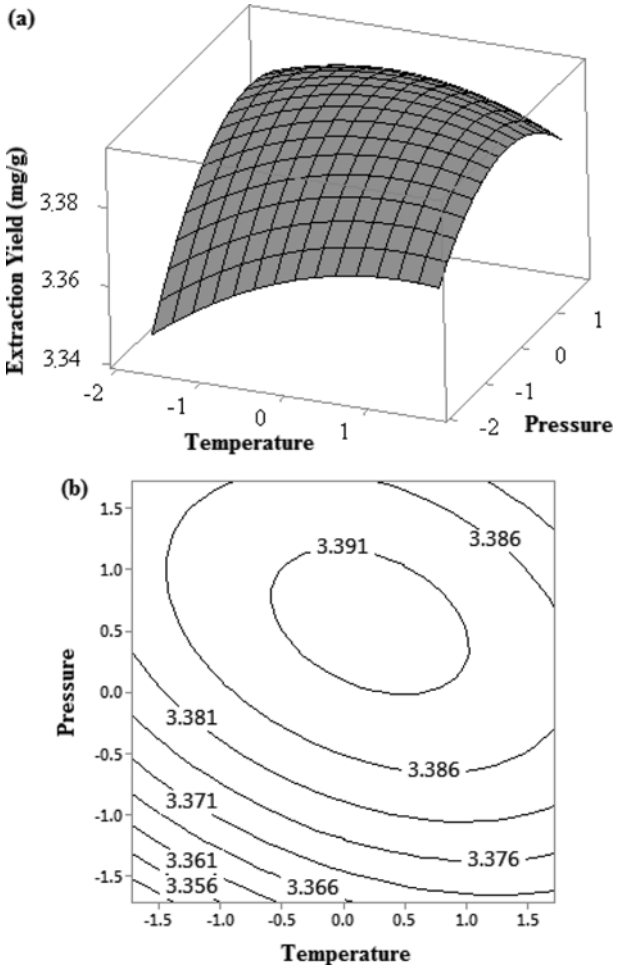

Fig. 8. The effects of temperature and pressure (coded values) on the galegine yield at dynamic extraction time of 90 min and CO_2 flow rate of 1.5 mL/min, (a) response surface plot, (b) contour plot.

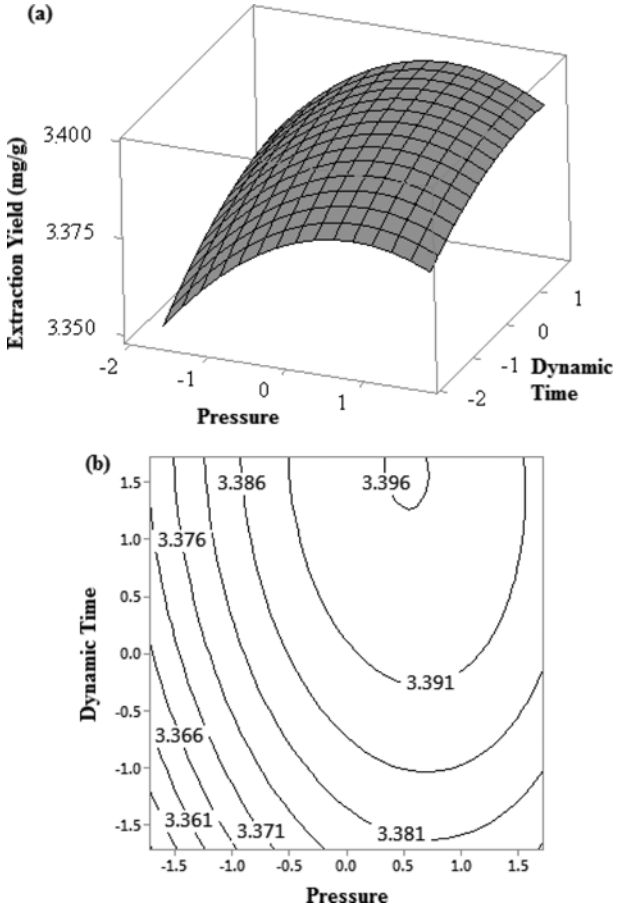

Fig. 9. The effects of pressure and dynamic extraction time (coded values) on the galegine yield at temperature of 45 °C and CO_2 flow rate of 1.5 mL/min, (a) response surface plot, (b) contour plot.

nal mass transfer coefficient and concentration gradient increase by increasing CO_2 flow rate. Thus, the use of a more rapid supply of fresh CO_2 into the extractor has direct effect on Reynolds number and consequently on Sherwood number used to calculate external mass transfer coefficient; and sweeps off the boundary layer surrounding plant particles, which raises mass transfer driving forces. But at high mass flow rates by decreasing contact time between SC-CO_2 and particles, the solubility of solute and then the yield will decline.

Increasing the SC-CO_2 flow rate from 0.5 mL/min (code=−1.72) to 2.15 mL/min (code=−0.5038) at the optimum conditions reduced the film thickness around the solid particles and resulted in lower external mass transfer resistance around the plant particles, and consequently enhanced galegine extraction yield. But at flow rates beyond 2.15 mL/min to 3 mL/min (code=2.5), the negative effect of lower residence time (i.e., fluid-bed contact time) dominated the positive effect of higher film mass transfer coefficient.

As depicted in Table 3, CO_2 had an insignificant linear positive effect and a highly significant quadratic negative effect. The interaction effect between flow rate and dynamic time was also highly significant (negative).

3-4. Effect of Dynamic Extraction Time

The effect of dynamic extraction time on the extraction yield is shown in Figs. 6, 9 and 11. Passing fresh solvent through *Galega officinalis L.* fixed bed was increased by increasing dynamic time of extraction, which improved the galegine extraction yield until there was effective mass transfer driving force between the SC-CO_2 and plant leaves.

According to Table 3, the dynamic extraction time had a highly significant positive linear effect on galegine recovery up to optimum dynamic time of 141.5 min ($p<0.001$). But, beyond 141.5 min (code= 1.72) the mass transfer driving force was gradually eliminated and therefore no more recovery enhancement was observed.

Fig. 12 shows interaction plots of operating variables for galegine yield, which represents all effects mentioned in above sections.

4. Modeling with ANN

MLP network with one hidden layer and six neurons in the hidden layer using LM (Levenberg-Marquardt backpropagation) training algorithm was selected for the supercritical extraction process modeling [55,56].

In a neural network, the connections (between inputs, hidden and output layers) consist of weights and biases. Then, the weighted output is passed through a transfer function. The initial weights matrix

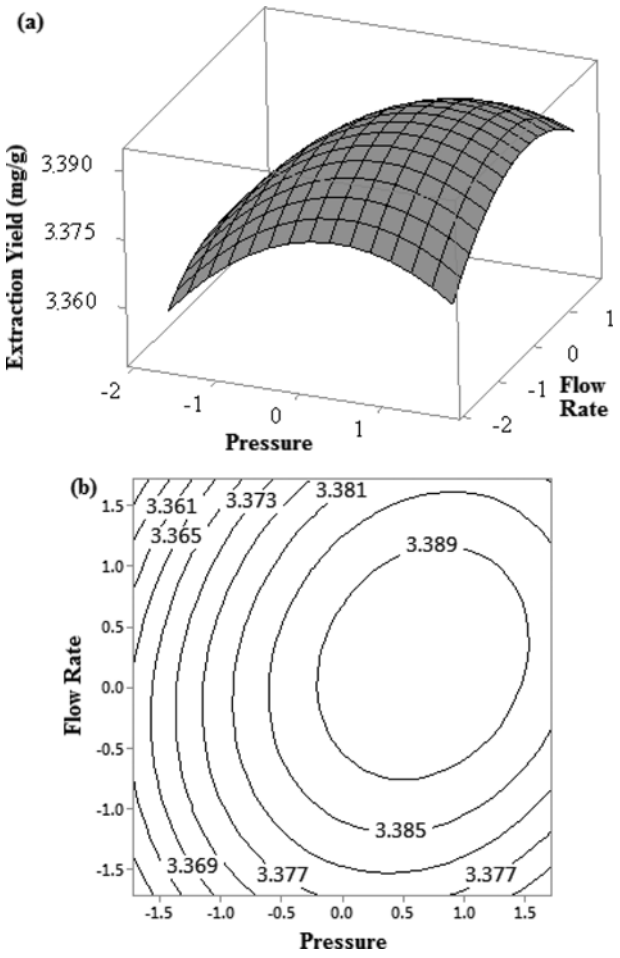

Fig. 10. The effects of CO_2 flow rate and pressure (coded values) on the galegine yield at temperature of 45 °C and dynamic extraction time of 90 min, (a) response surface plot (b) contour plot.

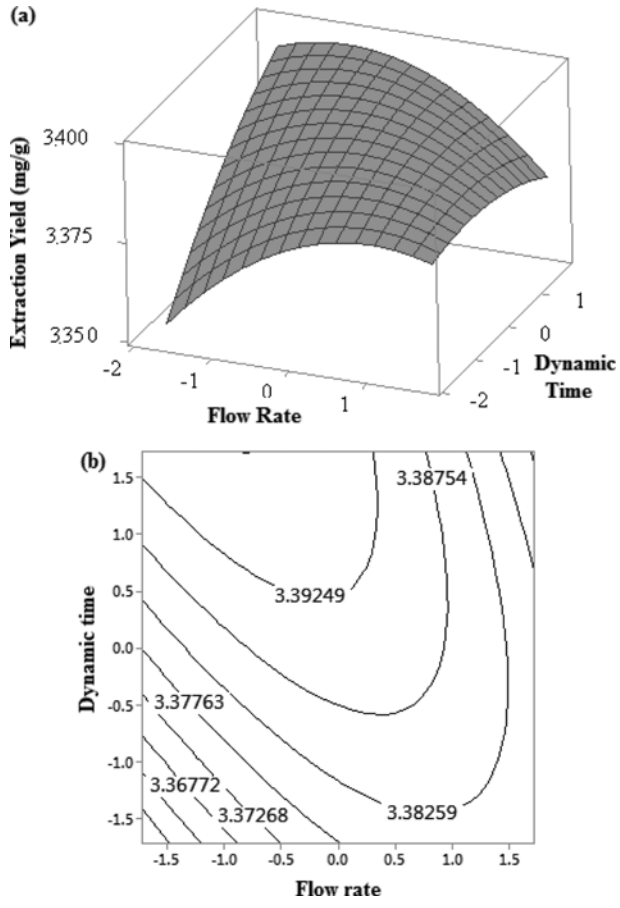

Fig. 11. The effects of CO_2 flow rate and dynamic extraction time (coded values) on the galegine yield at temperature of 45 °C and pressure of 20 MPa, (a) response surface plot, (b) contour plot.

and the biases were as follows:

$$iw\{1,1\} = \begin{bmatrix} -4.2355 & 0.11949 & -0.22407 & -0.94672 \\ 0.70611 & 3.6796 & -1.4552 & 0.99905 \\ 1.1972 & -0.8299 & -3.8902 & -3.7902 \\ -0.22436 & -1.9904 & -0.058003 & -0.42761 \\ 2.4283 & 0.48086 & 0.26783 & 0.6974 \\ -0.34849 & 0.9709 & 0.10332 & 2.1212 \end{bmatrix}$$

$$iw\{2,1\} = [-0.13252 \ -0.49587 \ 0.26071 \ -0.68289 \ 0.67506 \ 0.45043]$$

$$b\{1\} = \begin{bmatrix} 4.1121 \\ -0.77783 \\ 1.6052 \\ -0.60493 \\ 2.3505 \\ -0.27267 \end{bmatrix}$$

$$b\{2\} = [-0.27267]$$

Table 4. ANOVA results for the fitted quadratic polynomial model of SCF extraction

Source	Degree of freedom	Adjusted sum of squares	Adjusted mean squares	*F*-value	*p*-Value
Regression	14	32.1720	2.29800	16.28	0.000
Linear	4	15.4290	3.85726	27.32	0.000
Square	4	9.4219	2.35548	16.69	0.000
Interaction	6	7.3211	1.22018	8.64	0.000
Residual error	16	2.2587	0.14117	-	-
Lack-of-fit	10	2.2403	0.22403	73.05	0.000
Pure error	6	0.0184	0.00307	-	-
Total	30	34.43	-	-	-

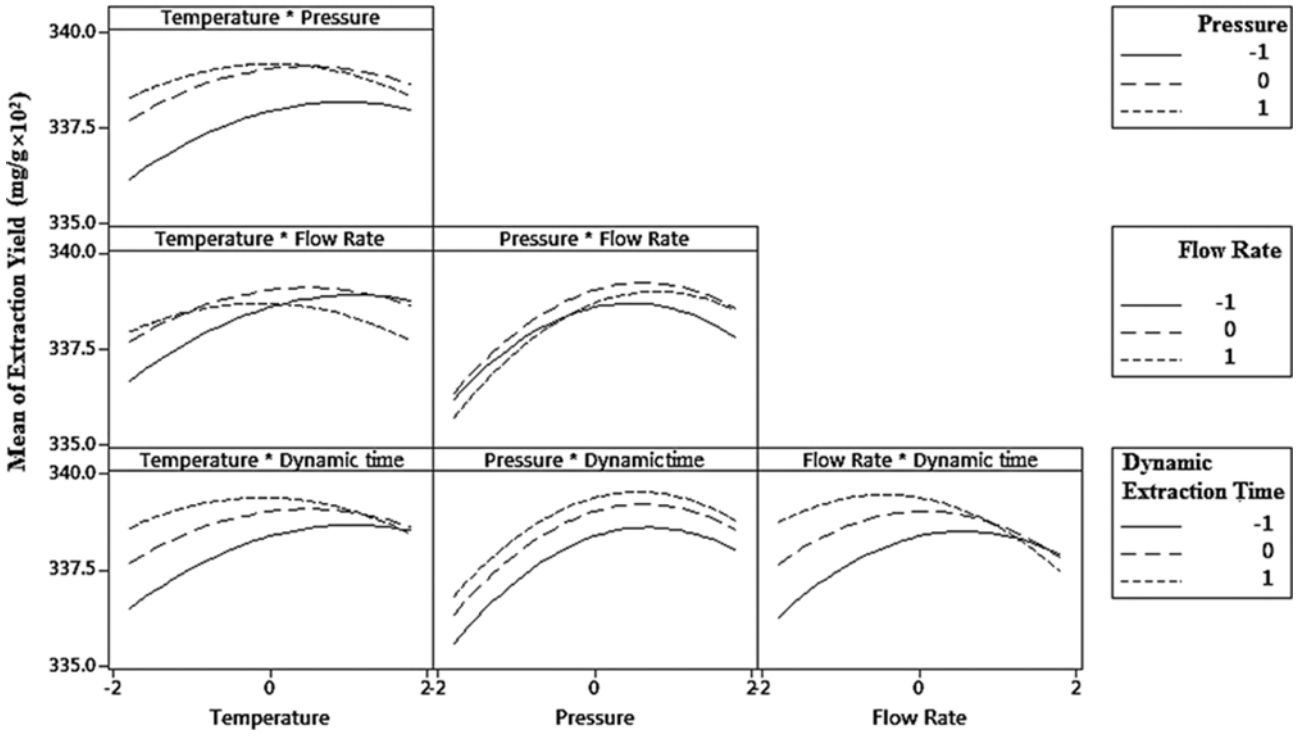

Fig. 12. Interaction plots for galegine yield based on response surface methodology.

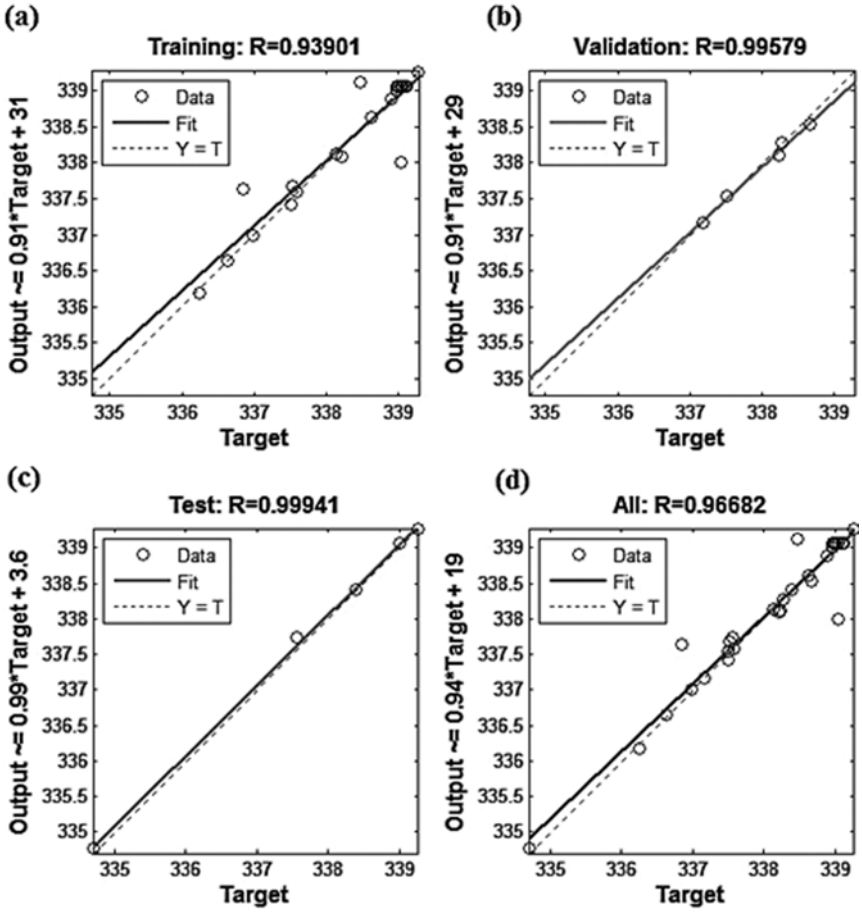

Fig. 13. Scatter plots of experimental data versus ANN modeling: (a) training, (b) validation, (c) testing, (d) all data.

Fig. 13 illustrates the scatter diagrams that compare the experimental data versus the computed neural network modeling data (for training, validation, testing and all data points).

The coefficient of determination (R^2) was 96.6%, which demonstrates very good compatibility between the experimental results and ANN calculated data.

CONCLUSIONS

Supercritical fluid extraction (SFE) using carbon dioxide was used for galegine extraction from *G. officinalis L.* due to its short extracting time, high extraction efficiency, lower refining requirement and failure to appear of chemical residues or contamination in the extracted products. The ANOVA in RSM modeling demonstrated all linear, quadratic, and interactions terms of process parameters (temperature, pressure, flow rate, and extraction time) except the linear term of flow rate; the quadratic term of extraction time as well as pressure-flow rate interaction and pressure-extraction time interaction, significantly affected extraction efficiency. The optimum conditions for the highest extraction yield of galegine (3.3932 (mg/g)) selected by the response surface methodology were as follows: T= 42.8 °C, P=22.7 MPa, F=2.15 mL/min, and t=141.5 min. ANN was developed to predict galegine extraction yield from *Galega officinalis L.* The coefficients of determination (R^2) in ANN modeling and RSM modeling were obtained to be 96.68% and 93.4%, respectively, which shows more accurate prediction using ANN modeling.

ACKNOWLEDGEMENTS

The financial support provided by Isfahan University of Technology is gratefully acknowledged.

REFERENCES

1. S. M. K. Rates, *Toxicon*, **39**, 603 (2001).
2. D. Egamberdieva, G. Berg, K. Lindström and L. A. Räsänen, *Plant Soil*, **369**, 453 (2013).
3. T. Fukunaga, K. Nishiya, K. Takeya and H. Itokawa, *Chem. Pharm. Bull.*, **35**, 1610 (1987).
4. H. R. Rasekh, P. Nazari, M. Kamli-Nejad and L. Hosseinzadeh, *J. Ethnopharmacol.*, **116**, 21 (2008).
5. P. G. Peiretti and F. Gai, *Anim, Feed Sci. Technol.*, **130**, 257 (2006).
6. L. A. Witters, *J. Clin. Invest.*, **108**, 1105 (2001).
7. P. Palit, B. L. Furman and A. I. Gray, *J. Pharm. Pharmacol.*, **51**, 1313 (1999).
8. K. Pundarikakshudu, J. K. Patel, M. S. Bodar and S. G. Deans, *J. Ethnopharmacol.*, **77**, 111 (2001).
9. M. Trojan-Rodrigues, T. L. S. Alves, G. L. G. Soares and M. R. Ritter, *J. Ethnopharmacol.*, **139,** 155 (2012).
10. A. T. Atanasov, *Phytother. Res.*, **8**, 314 (1994).
11. M. H. Mooney, S. Fogarty, C. Stevenson, A. M. Gallagher, P. Palit, S. A. Hawley, D. G. Hardie, G. D. Coxon, R. D. Waigh, R. J. Tate and A. L. Harvey, *Br. J. Pharmacol.*, **153**, 1669 (2008).
12. C. R. Huxtable, P. R. Dorling and S. M. Colegate, *Aust. Vet. J.*, **70**, 169 (1993).
13. V. Spasov, *Bulg. J. Vet. Med.*, **6**, 203 (2003).
14. K. A. Wadkar, C. S. Magdum, S. S. Patil and N. S. Naikwade, *J. Herb. Med. Tox.*, **2**, 45 (2008).
15. I. Vermaak, A. M. Viljoen and J. H. Hamman, *Nat. Prod. Rep.*, **28**, 1493 (2011).
16. D. S. Fabricant, D. Nikolic, D. C. Lankin, S. N. Chen, B. U. Jaki, A. Krunic, R. B. van Breemen, H. H. Fong, N. R. Farnsworth and G. F. Pauli, *J. Nat. Prod.*, **68**, 1266 (2005).
17. F. González-Andrés, P. A. Redondo, R. Pescador and B. Urbano, *N. Z. J. Agric. Res.*, **47**, 233 (2004).
18. T. A. Azhunova and P. V. Markizov, *Pharm. Chem. J.*, **28**, 410 (1994).
19. W. J. Kim, C. H. Choi and S. H. Moon, *Korean J. Chem. Eng.*, **19**, 617 (2002).
20. P. K. Ghosh and P. Bhattacharjee, *Korean J. Chem. Eng.*, **33**, 1681 (2016).
21. L. Tian, M. Zhou, X. Pan, G. Xiao and Y. Liu, *Korean J. Chem. Eng.*, **32**, 1649 (2015).
22. R. Kasirajan, S. Pandian, S. Tamilarasan and R. Sahadevan, *Korean J. Chem. Eng.*, **31**, 509 (2014).
23. S. Ferdosh, M. Z. I. Sarker, N. N. N. Ab Rahman, M. J. H. Akand, K. Ghafoor, M. B. Awang and M. O. Ab Kadir, *Korean J. Chem. Eng.*, **30**, 1466 (2013).
24. A. Hedayati and S. M. Ghoreishi, *J. Supercrit.*, **100**, 209 (2015).
25. S. M. Ghoreishi, S. M. Mortazavi and A. Hedayati, *Chem. Prod. Process Model.*, **10**, 243 (2015).
26. S. M. Ghoreishi, A. Hedayati and M. Kordnejad, *J. Supercrit.*, **111**, 162 (2016).
27. S. M. Ghoreishi, A. Hedayati and K. Ansari, *J. Supercrit.*, **117**, 131 (2016).
28. A. Ali-Nehari and B. S Chun, *Korean J. Chem. Eng.*, **29**, 918 (2012).
29. A. Ali-Nehari, S. B. Kim, Y. B. Lee, H. Y. Lee and B. S. Chun, *Korean J. Chem. Eng.*, **29**, 329 (2012).
30. S. M. Ghoreishi, A. Hedayati and S. Mohammadi, *J. Supercrit.*, **113**, 53 (2016).
31. K. Y. Kang, D. H. Ahn, G. T. Wilkinson and B. S. Chun, *Korean J. Chem. Eng.*, **22**, 399 (2005).
32. C. H. Lee, Y. W. Lee, J. D. Kim and K. H. Row, *Korean J. Chem. Eng.*, **18**, 352 (2001).
33. A. Hedayati and S. M. Ghoreishi, *Chem. Prod. Process Model.*, **11**, 217 (2016).
34. A. J. Jafari, B. Kakavandi, R. R. Kalantary, H. Gharibi, A. Asadi, A. Azari, A. A. Babaei and A. Takdastan, *Korean J. Chem. Eng.*, **33**, 2878 (2015).
35. Y. H. Chu, I. S. Han and C. Han, *Korean J. Chem. Eng.*, **19**, 535 (2002).
36. M. Sedighi, K. Keyvanloo and J. Towfighi, *Korean J. Chem. Eng.*, **27**, 1170 (2010).
37. B. Zarenezhad and A. Aminian, *Korean J. Chem. Eng.*, **28**, 1286 (2011).
38. E. M. E. M. Shokir, E. S. Al-Homadhi, O. Al-Mahdy and A. A. H El-Midany, *Korean J. Chem. Eng.*, **31**, 1496 (2014).
39. S. Murugesan, S. Rajiv and M. Thanapalan, *Korean J. Chem. Eng.*, **26**, 364 (2009).
40. M. Moradi, F. Ghanbari, M. Manshouri and K. A. Angali, *Korean J. Chem. Eng.*, **33**, 539 (2016).
41. S. K. Cho, D. H. Kim, Y. M. Yun, K. W. Jung, H. S. Shin and S. E. Oh, *Korean J. Chem. Eng.*, **30**, 1493 (2013).

42. M. G. Goleroudbary and S. M. Ghoreishi, *J. Supercrit.*, **108**, 136 (2016).
43. A. I. Khuri and S. Mukhopadhyay, *Wiley Interdiscip. Rev. Comput. Stat.*, **2**, 128 (2010).
44. H. Su, X. Wang, Y. G. Kim, S. B. Kim, Y. G. Seo, J. S. Kim and C. J. Kim, *Korean J. Chem. Eng.*, **31**, 2070 (2014).
45. F. Bashipour and S. M. Ghoreishi, *J. Supercrit.*, **95**, 348 (2014).
46. S. C. Wang, *Artificial neural networ*k. *In Interdisciplinary Computing in Java Programming*, Springer US, 81-100 (2003).
47. D. M. Himmelblau, *Korean J. Chem. Eng.*, **17**, 373 (2000).
48. S. M. Ghoreishi, A. Hedayati and S. O. Mousavi, *J. Supercrit.*, **112**, 57 (2016).
49. A. A. Khadom, *Korean J. Chem. Eng.*, **30**, 2197 (2013).
50. J. O. Valderrama, J. M. Muñoz and R. E. Rojas, *Korean J. Chem. Eng.*, **28**, 1451 (2011).
51. Z. İlbay, S. Şahin and K. Büyükkabasakal, *Korean J. Chem. Eng.*, **31**, 1661 (2014).
52. L. Fausett, *Fundamentals of neural networks: architectures, algorithms, and application*, Prentice-Hall, Inc. (1994).
53. I. A. Basheer and M. Hajmeer, *J. Microbiol. Methods*, **43**, 3 (2000).
54. V. Kůrková, *Neural Net.*, **5**, 501 (1992).
55. N. Chandrakar, *Korean J. Chem. Eng.*, **33**, 1318 (2016).
56. A. A. Babaei, A. Khataee, E. Ahmadpour, M. Sheydaei, B. Kakavandi and Z. Alaee, *Korean J. Chem. Eng.*, **33**, 1352 (2016).